Results in Surfaces and Interfaces 14 (2024) 100183

Contents lists available at ScienceDirect

Results in Surfaces and Interfaces

journal homepage: www.elsevier.com/locate/rsurfi

Silane modified clay for enhanced dye pollution adsorption in water

Marlène Huguette Tsaffo Mbognou [a,b,c], Stéphanie D. Lambert [a], Ernestine Mimba Mumbfu [c], Joachim Caucheteux [a], Antoine Farcy [a], Nathalie Fagel [d], Emmanuel Djoufac Woumfo [b], Julien G. Mahy [a,e,*]

[a] Department of Chemical Engineering – Nanomaterials, Catalysis & Electrochemistry, University of Liège, B6a, Quartier Agora, Allée du Six Août 11, 4000, Liège, Belgium
[b] Laboratoire de Physico-Chimie des Matériaux Minéraux, University of Yaounde I, 337, Yaounde, Cameroon
[c] Institute of Geological and Mining Research (IRGM), 4110, Yaounde, Cameroon
[d] Laboratoire Argiles, Géochimie et Environnements Sédimentaires (AGEs), Department of Geology, Faculty of Sciences, University of Liège, Liège, B-4000, Belgium
[e] Institut National de la Recherche Scientifique (INRS), Centre-Eau Terre Environnement, Université du Québec, 490, Rue de La Couronne, Québec (QC), G1K 9A9, Canada

ARTICLE INFO

Keywords:
Silicon alkoxides
Porous material
Water treatment
Pollution removal
Hybrid compounds

ABSTRACT

A natural clay from Bakotcha in Cameroon was modified with two silanes, tetramethoxysilane (TMOS) and [3-(2-aminoethyl)aminopropyl]trimethoxysilane (EDAS) to increase its adsorption properties. The modified clay is intended to be used as an efficient adsorbent for organic pollutant removal from water. Three Clay/TMOS and two Clay/EDAS samples with different [silane]/[clay] ratios were produced and characterized by X-ray diffraction, N_2 adsorption-desorption measurements, Inductively Coupled Plasma–Atomic Emission Spectroscopy and Scanning Electron Microscopy. Their adsorption properties were evaluated on three organic model pollutants (i.e. fluorescein, malachite green and brilliant violet diamond). A dilution of the montmorillonite structure of the raw clay is observed when it is modified with TMOS while its original crystalline structure is preserved with EDAS. The morphologies depended on the used silane: (i) with TMOS, highly porous materials with the formation of silica particles at the surface of the clay; (ii) with EDAS, a similar morphology as raw clay with EDAS grafted at the surface of the clay. Both morphologies give two different adsorption behaviors on the 3 pollutants. For the raw clay and the TMOS modified clays, similar adsorption properties are obtained with a better adsorption when the specific surface increases (when TMOS content increases). When clay is modified with EDAS, the adsorption properties change as the surface groups are different, these EDAS modified samples have less affinity with fluorescein and malachite green reducing the adsorption capacity for this kind of pollutants. The tuning of the raw clay with silane opens the way for the development of highly efficient adsorbent for pollutants in water from natural and inexpensive materials.

1. Introduction

Silicates belonging to the clay mineral family are increasingly studied as an important class of solids that can yield nanostructured materials with interesting properties as hydrophobicity, hydrophilicity, biocompatibility or as building block for more complex structures (Dong and Zhang, 2018; Zhou et al., 2016). Studies focused on the functionalization of clay materials to obtain hybrid compounds where inorganic and organic components are linked by covalent and ionic-covalent bonds. This research is focused on achieving a high percentage of clay sheet exfoliation in polymer matrices by improving the interactions between clay surfaces and polymer chains through various surface modification approaches (Viville et al., 2004).

There exist many attractive characteristics on clay surfaces, such as hydroxyl groups on the edges, silanol groups of crystal defects, providing surface modification and functionalization strategies. The common method used to modify the surface of clays is cation exchange reaction with alkylammonium (Viville et al., 2004; Park et al., 2005). This increases the interlayer space and creates a favorable organophilic environment (Viville et al., 2004; Park et al., 2005).

A novel modification approach involving a direct grafting reaction to form covalent bonds on clay surfaces has attracted much attention

* Corresponding author. Allée du Six Août 11, 4000 Liège, Belgium.
E-mail address: julien.mahy@uliege.be (J.G. Mahy).

https://doi.org/10.1016/j.rsurfi.2024.100183
Received 30 August 2023; Received in revised form 29 December 2023; Accepted 10 January 2024
Available online 12 January 2024

(Wheeler et al., 2005; He et al., 2005). The organosilanes were covalently bound to the clay surfaces via a condensation reaction with the surface silanol groups (Si–OH), resulting in closer interactions between the organic components and the clay than ionic interaction and physical adsorption (Tonle et al., 2003; He et al., 2013). Indeed, since a few years, silicon alkoxides are used either to modify the textural properties of inorganic materials used as catalysts in gaseous phase (Lambert et al., 2008; Claude et al., 2019; Mahy et al., 2017), or to play the role of link between organic molecules and inorganic photocatalytic materials (Mahy et al., 2019a, 2023).

Functionalizing swelling aluminosilicate clays of the smectite type, such as montmorillonite, would generally result in limited amounts of –OH groups (Celis et al., 2000; Song and Sandi, 2001). For grafting organic ligands onto the interlamellar surface of such clays, the literature is sparse, and the resulting materials may suffer from impeded access to binding sites, as shown by less than complete adsorption of heavy metal species relative to the total number of ligands (Mercier and Pinnavaia, 1998).

To overcome the limitation of the surface grafting modification method, the sol-gel route is used to synthesize organoclay using silicon alkoxides as the priority source of silica. Carrado et al. (Carrado, 2000) provided an approach that allows a large amount of silanes to covalently attach to the clay surface due to the *in-situ* process and more silanol moieties. Nevertheless, the high degree of organosilane incorporation is often accompanied by distortions and structural defects (Qian et al., 2008).

These modifications allow the formation of hybrid materials with increased adsorption properties for pollutant removal. Indeed, with the expansion of industries during the past two centuries, pollution has increased greatly all around the world and the development of depollution techniques using inexpensive materials became essential (Kemgang Lekomo et al., 2021; Shayesteh et al., 2015; Paredes-Quevedo et al., 2021). Natural clay represents an inexpensive material, available in a lot of developing countries, that can be a good candidate for organic pollutant adsorption from water (Srivastava et al., 2009; Akçay et al., 2009; Nodehi et al., 2020; Tchanang et al., 2021; Queiroga et al., 2019, 2021; De Queiroga et al., 2019).

The objectives of this work are to explore the possibilities of using natural Cameroonian clays as raw material for the preparation of organic-inorganic hybrid compounds by grafting with silanol groups, i.e. either tetramethoxysilane (TMOS) or [3-(2-aminoethylamino)propyl] trimethoxysilane (EDAS), using a well-controlled and easy sol-gel procedure. The resulting nanocomposite materials are evaluated as adsorbents for dyes such as fluorescein, malachite green and brilliant purple diamond present in water polluted by textile industries. The experiments are performed with raw clays from the locality of Bakotcha (West Cameroon). Several physico-chemical techniques were used to evaluate the efficiency of the functionalization process.

2. Material and methods

2.1. Clay material and chemical reagents

A smectite type clay material from the locality of Bakotcha, (West Cameroon) was used in this work. It corresponds to a montmorillonite clay with trace of cristobalite and feldspars as shown by the X-ray diffractogram in (Mahy et al., 2022). The sampled clay was air-dried in the laboratory to a constant weight before grinding and sieving in a 160 μm diameter sieve. The silica precursors and the solvent were tetramethoxysilane (TMOS, 98%, density = 1.032 g/mL) from Alfa Aesar, [3-(2-aminoethyl)aminopropyl]trimethoxysilane (EDAS, 80%, density = 1.028 g/mL) from Sigma Aldrich, Ethanol absolute (ACS grade) from Merck. Hydrochloric acid (HCl 36–38%, Merck) was used to adjust the pH of the solution. All solutions were prepared with deionized water.

2.2. Sol-gel method to modify clay with alkoxides

Clays modified with organosilanes were prepared by sol-gel process either to saturate the material with silica (TMOS) or graft amine groups (EDAS). The synthesis used was inspired from (Qian et al., 2008). Different alkoxide/clay mass ratios were taken in order to evaluate the influence of the reagent composition. Table 1 represents the different ratios.

2.2.1. TMOS modified clay samples

50 mL of deionized water was acidified with hydrochloric acid (36–38%, Merck) to pH 1.5 and put under magnetic stirring at room temperature. A weight of 3.10 g of montmorillonite clay was added to the initial solution under continuous stirring. Specific amount of TMOS, depending to the aimed ratio (Table 1), was taken and introduced into 10 mL of absolute ethanol. This second mixture was added to the initial solution under stirring at 25 °C until a light brown sol was formed. The gel is aged in an oven for condensation for 24 h at 25 °C and finally dried at 60 °C for 48 h. The procedure used is called acid-catalyzed procedure because the acid catalyzes the sol-gel process (Brinker and JeffreyScherer, 2013).

2.2.2. EDAS modified clay samples

The syntheses of samples with EDAS were similar to the ones with TMOS, except that the gel was aged for 3 days in an oven at 80 °C for condensation and finally dried at 150 °C for 24 h. Only two ratios were synthesized since the clay/EDAS ratio 3/10 was too viscous that it was impossible to dry and work with it.

2.3. Material characterization methods

Nitrogen adsorption-desorption isotherms of all samples were determined in an ASAP multisampler device from Micromeritics at −196 °C. The samples were degassed at 120 °C for 24 h before analysis.

X-ray diffraction (XRD) patterns were recorded on a Bruker D8 Twin-Twin powder diffractometer (Bruker, Billerica, MA, USA) using Cu-Kα radiation, with a step size of 0.002°, a scan speed of 2°/min, a 2 theta range of 2–70°, a current of 40 mA, and a voltage of 40 kV. Phase quantification was made with TOPAS software.

Fourier transform infrared (FTIR) spectra in the region of 400–4000 cm^{-1} are recorded at room temperature with a Thermo Nicolet Nexus FTIR spectrometer (Laboratoire de Minéralogie, ULiège). All catalyst powders are dispersed in KBr (1 wt % for all samples).

The zeta potential is measured on the different sample suspensions with a DelsaNano C device from Beckman Coulter.

The point of zero charge (PZC) is evaluated for each sample as follows (Schreier and Regalbuto, 2004): 11 vials are prepared with 10 mL of Milli-Q water. The pH of each of these vials is adjusted with diluted HCl and NaOH solutions to cover a pH range of 2–12 with a ΔpH of 1 between each vial. Then, an equal amount of sample is placed in each of the vials. The mass of sample to be added must be such that the surface concentration in a vial is 1000 $m^2\ L^{-1}$, i.e. a specific surface area of 10 m^2 in 10 mL. Once the sample is suspended in each vial, they are stirred for 1 h. After this time, the pH of each of the vials is measured again and a graph of the final pH versus the initial pH can be drawn. The PZC is given by the pH value at which a plateau appears on the graph (Schreier and Regalbuto, 2004).

Scanning electron microscopy (SEM) pictures were obtained on a

Table 1
Clay/TMOS and Clay/EDAS mass ratios.

Ratio Clay/TMOS (w/w)	Ratio Clay/EDAS (w/w)
3/3	3/3
10/3	10/3
3/10	–

TESCAN CLARA microscope operating at 15 keV.

The actual composition of the clay materials was determined by Inductively Coupled Plasma–Atomic Emission Spectroscopy (ICP–AES), equipped with an ICAP 6500 THERMO Scientific device. The mineralization is fully described in (Mahy et al., 2016) with HF used instead of HNO_3.

2.4. Adsorption experiments

The adsorption tests were evaluated on the raw clay material and on the TMOS and EDAS functionalized clay samples with the different mass ratios (6 samples in total). Three model pollutants and dyes used in the pesticide and textile industries, were tested: malachite green (MG, pKa 6.9), fluorescein (FL, pKa 6.4) and brilliant violet diamond (BVD, Remazol brilliant violet 5R, pKa not referenced in literature). Six vials containing sample powders of 5, 10, 15, 20, 25 and 30 mg with 20 mL of pollutant solution in water were prepared for adsorption experiment. Initial solution concentrations of pollutants were 20 mg/L for FL (pH = 5.3) and 4 mg/L for MG (pH = 6.2) and BVD (pH = 7.2), these pollutant concentrations are commonly found in adsorption studies on this kind of molecules (Shayesteh et al., 2015; Nodehi et al., 2020; Tchanang et al., 2021). The different samples were shaken continuously in the dark. Aliquots of pollutants were taken every 10, 20, 60 min up to 2 h. Residual concentrations of pollutants were assessed with a Genesis 150S UV–Vis spectrophotometer (Thermo Scientific) without filtration. Previously, calibration curves were made for each pollutant. The main adsorption peaks were located at 485 nm for fluorescein, 550 nm for brilliant violet diamond and 660 nm for malachite green.

3. Results and discussion

3.1. Composition of modified clays

Silica-clay nanocomposites were prepared at different ratios as described in the experimental section (section 2.2). Variable amounts of silicon alkoxysilanes (TMOS and EDAS) mixed with ethanol were slowly added to dispersions of clays acidified with hydrochloric acid. Each mixture was homogenized under continuous stirring at room temperature. HCl was added to allow TMOS or EDAS to be covalently bound to the surface of the clays so that it could react with other hydrolyzed molecules of the same type. Depending on the amount of TMOS or EDAS added, gelation of the system occurred. The gel formed in the Clay/TMOS 3/10 case does not have a high viscosity. TMOS contributes to a reaction gelation time between 30 min and 2 h for the 3/10 Clay/silane ratio. When EDAS is used, there is no gelation of the samples. The Clay/EDAS (3/10) sample did not yield any powder product after drying; the gel remained soft. The different capacities of silanes to insert themselves into the clay sheets could explain these observations. Diffusion is facilitated by the lower steric hindrance presented by TMOS (small molecular size) compared to EDAS. The condensation step is slower when the number of silanol groups on the alkoxysilane is smaller (He et al., 2005). The surfaces of the clays were fixed by silane arrays or silica nanoparticles depending on the Clay/TMOS or Clay/EDAS ratio (Qian et al., 2008).

The Al and Si composition measured by ICP-AES is given in Table 2.

Table 2
Al and Si compositions of all samples measured by ICP.

Sample	Al (wt%)	Si (wt%)	Si/Al
Raw clay	11.4	20.7	1.82
Clay/TMOS 3/10	9.74	21	2.16
Clay/TMOS 3/3	7.24	23.4	3.23
Clay/TMOS 10/3	10.2	22.7	2.23
Clay/EDAS 3/3	7.82	19.9	2.54
Clay/EDAS 10/3	10.5	22	2.10

The addition of silane increases the amount of silicon in the sample and the ratio Si/Al increases. TMOS/Clay samples contain more silicon than EDAS/Clay samples.

FTIR spectroscopy was applied to analyze possible differences in samples (Fig. 1). The FTIR spectrum of the raw Clay (Fig. 1a or 1b in blue) shows the following characteristic bands (Madejova'and et al., 2001): at 3650 cm^{-1}, stretching vibrations of the OH bonds that correspond to hydroxyl groups of the montmorillonite structure; at 3590 cm^{-1}, tension vibrations of the OH bonds of the chemisorbed and physisorbed water; and at 1610 cm^{-1}, the deformation vibration of the OH bonds. The band at 1020 cm^{-1} results from the stretching vibration of the Si–O bonds of the Montmorillonite (Mt) structure (Slaný et al., 2019). In addition, the band at 790 cm^{-1} corresponds to the deformation vibration of the Si–O bonds of silica, which is an associated phase. The bands at 909 cm^{-1}, result from the deformation vibrations of the Al–OH bonds of the AlAlOH structural groups. The band at 620 cm^{-1} is assigned to the coupling vibrations of the Al–O and Si–O groups of the Mt structure and the bands at 520 cm^{-1} and 490 cm^{-1} correspond to the deformation vibrations of the Al–O–Al and Si–O–Si groups, respectively.

The FTIR spectra of natural clay and modified ones are all presented in Fig. 1. Surface modification of montmorillonite with TMOS and EDAS was demonstrated by FTIR. Indeed, the asymmetric stretching modes of Si–O–Si were observed at 40 and 1020 cm^{-1} while the stretching vibrations of Al–O–Si were observed at 790 and 520 cm^{-1} for every TMOS and EDAS samples (Fig. 1a and b). The hydroxyl group bound to aluminum (Al(Al)OH) or magnesium (Al(Mg)OH) shows stretching vibrations at 3690 cm^{-1}. The stretching of the hydroxyl group and bending vibrations of the H–O–H bonds in the adsorbed water molecules intercalated in the clay mineral occur approximately at 3465 cm^{-1} and 1630 cm^{-1} respectively (Piscitelli et al., 2012). However, the latter was shifted to 1630 cm^{-1} in the amino-functionalized clay mineral (Fig. 1b). The new absorption band at 2950 cm^{-1} corresponds to the C–H stretching vibration of single bond CH_2 groups of EDAS (Fig. 1b). These FTIR bands indicate the surface modification of natural montmorillonite by silica alkoxides. New bands were observed at 1490 cm^{-1} and 1320 cm^{-1}, corresponding to single-bond NH_2 and Si–CH vibrations respectively, which also confirmed the presence of the silane (Fig. 1b).

3.2. Crystallinity

The XRD patterns of the different samples (Fig. 2) has allowed to estimate the crystalline structure of the samples. The raw cay is characterized by the following minerals: montmorillonite, talc, kaolinite, illite, feldspar, augite and cristobalite. The quantification of phases is presented in Table 3.

In the case of the Clay/TMOS sample series (Fig. 2), the intensity of the clay diffraction peaks decreases when the clay is modified with TMOS. It becomes practically nonexistent when the Clay/TMOS ratio is low (i.e. 3/10). This result suggests that the clay platelets were delaminated during the synthesis reaction (Qian et al., 2008) and that large amount of amorphous silica is introduced in the samples. Concerning the quantification of crystalline phases (Table 3), it is observed a decrease of three phases: kaolinite, illite and cristobalite. This modification of phases can be due to acid leaching during the modification of clay with the silane (Komadel and Madejová, 2006; Espínola et al., 2003). Indeed, it is made in acidic condition (HCl at pH of 1.5, see experimental section). For the sample Clay/TMOS 3/10, mainly montmorillonite is detected.

In the Clay/EDAS patterns (3/3) and (10/3) (Fig. 2), the peaks of the different minerals present in the raw material are still visible after the EDAS modification with similar intensities. This would mean that with the low proportion of EDAS used during the syntheses, its incorporation in the clay did not change the initial structure of the material. Concerning the quantification of crystalline phases (Table 3), it is also observed a decrease of three phases: kaolinite, illite and cristobalite. Similar explanation than samples modified with TMOS can be drawn

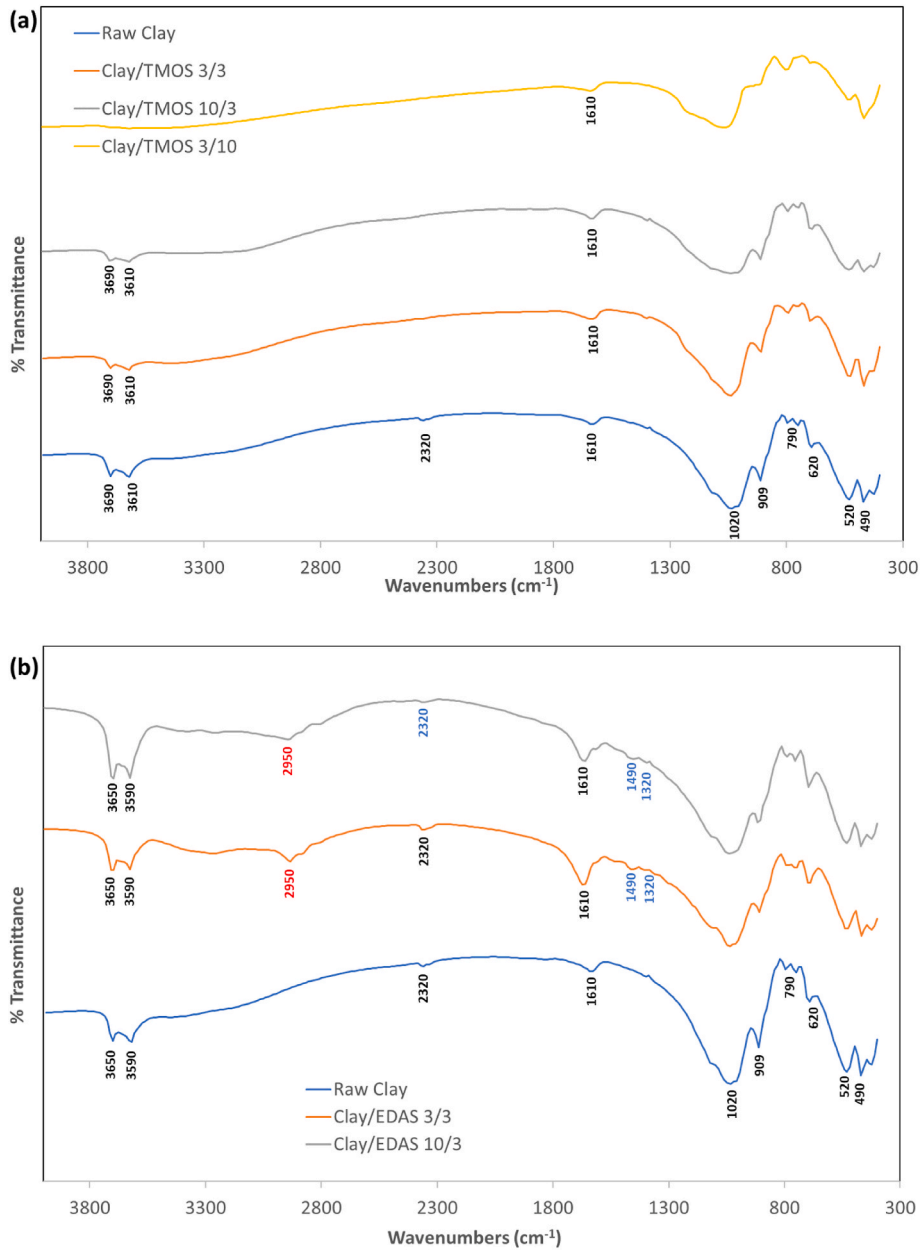

Fig. 1. FTIR spectra of the 6 samples: (a) TMOS series and (b) EDAS series.

due to the acidic treatment.

For all samples modified with silane (TMOS of EDAS), it is observed a modification of the pic located at 5.7° for the raw Clay. This peak corresponds to the basal spacing (001) and is related to the degree of intercalation of species in clay. According to (Asgari and Sundararaj, 2018), functionalization with silanes shifts the peak towards lower values of 2θ. The average value of (001) differs significantly depending on the medium used. This can be attributed to the high amounts of chemical grafting at the edges, which slightly separate the separated layers due to the richness of grafted species.

In (Piscitelli et al., 2010), X-ray diffraction patterns related to basal spacing (001), show that the introduction of any type of aminosilane into the Montmorillonite gallery shifts the peak to lower values compared to the bulk material. This increase in basal spacing is a clear signal that each aminosilane species has been grafted/intercalated into the Montmorillonite interplatelet space. In detail, pure MT sample shows a peak at 2 Θ equal to 7.5, while MT modified by aminosilane sample shows diffraction peaks at 2 Θ values between 5.3 and 5.9 (Piscitelli et al., 2010).

In the case of this study, the samples modified with EDAS have their basal peak modified from 5.7 for the raw Clay to 4.3 and 4.5 for the Clay/EDAS 3/3 and Clay/EDAS 3/10, respectively. It indicates an intercalation of the silane in the Montmorillonite structure.

Concerning the samples modified with TMOS, it is a displacement of the basal peak towards higher values (6.9, 7.1 and 6.6 for Clay/TMOS 3/10, Clay/TMOS 3/3, and Clay/TMOS 10/3, respectively). This indicates a different behavior with this silane (TMOS) compared to EDAS which leads to less spacing between the sheets of the Montmorillonite structure.

3.3. *Texture and surface aspect of samples*

The textural properties of samples were confirmed by nitrogen adsorption-desorption measurements. Table 4 shows the specific surface areas (S_{BET}), the microporous volume (V_{micro}) and the porous volume (V_P) of the different samples. The bare clay sample has a relatively low

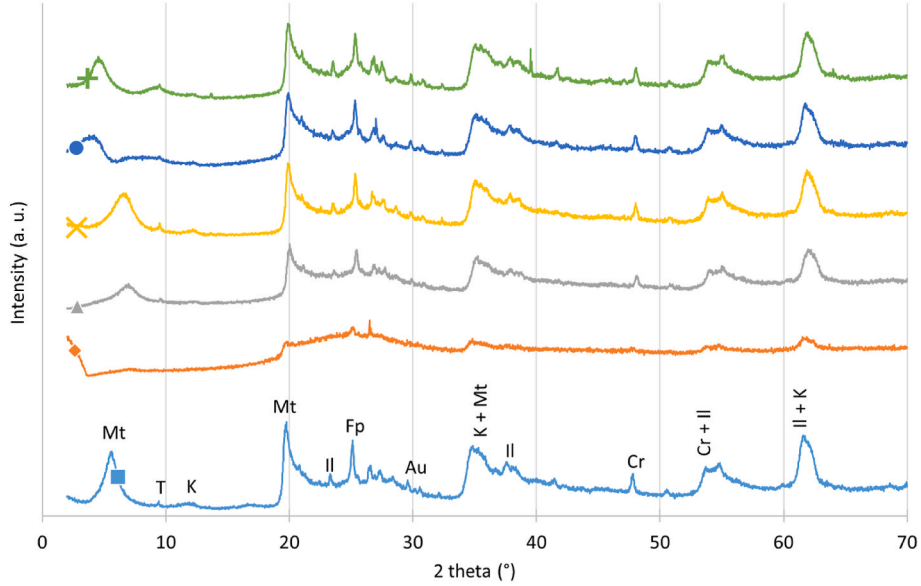

Fig. 2. XRD patterns of samples: (■) Raw Clay, (◆) Clay/TMOS 3/10, (▲) Clay/TMOS 3/3, (x) Clay/TMOS 10/3, (●) Clay/EDAS 3/3, and (+) Clay/EDAS 10/3. The positions of the reference peaks are indicated on the raw clay by the following letters: (Mt) montmorillonite, (T) talc, (K) kaolinite, (Il) illite, (Fp) feldspar, (Au) augite, and (Cr) cristobalite. The positions are not indicated on the composite materials to not overload the figure.

Table 3
XRD phase quantification with TOPAS software.

Samples	Montmorillonite (%)	Talc (%)	Kaolinite (%)	Illite (%)	Feldspar (%)	Augite (%)	Cristobalite (%)
Raw clay	80.22	2.01	4.19	7.58	0.52	0.85	4.64
Clay/TMOS 3/10	93.03	0.59	0	1.12	3.65	0.94	0.67
Clay/TMOS 3/3	83.87	0	1.1	2.24	5.13	3.13	4.54
Clay/TMOS 10/3	85.21	0	1.51	1.16	6.85	2.53	2.75
Clay/EDAS 3/3	84.1	0	1.02	3.23	5.78	3.1	2.78
Clay/EDAS 10/3	84.07	0	0.52	3.66	7.88	2.65	1.22

Table 4
Texture of samples.

Sample	S_{BET} (m^2/g) ±5	V_{micro} (cm^3/g) ±0.01	V_P (cm^3/g) ±0.01	Zeta potential (mV) ±0.01	pH of zeta potential (−)	PZC (−) ±0.1
Raw clay	45	0.03	0.07	−10.94	5.4	6
Clay/TMOS 3/10	660	0.30	0.39	−8.07	3.5	3.7
Clay/TMOS 3/3	285	0.14	0.20	+3.40	3.2	3.2
Clay/TMOS 10/3	135	0.07	0.12	+2.41	3.4	3.4
Clay/EDAS 3/3	55	0.02	0.03	+34.49	9.2	8.2
Clay/EDAS 10/3	55	0.02	0.04	+10.34	6.1	5.3

S_{BET}: specific surface area obtained by BET method; V_{micro}: microporous volume; V_p: specific liquid volume adsorbed at saturation pressure of nitrogen.

specific surface area (45 m^2/g), which increases highly when TMOS is used (between 135 and 660 m^2/g). This increase can be due to the production of micro-meso silica materials in the clay. In Fig. 2, the montmorillonite peak nearly disappears with the increase of TMOS amount used during the syntheses.

When EDAS is grafted, only a slight specific surface area increase is observed (around 55 m^2/g) and a reduction of the porous volume (Table 4). This increase is due to the intercalations of the silanes into the smectite lattice (Qian et al., 2008). This insertion is observed in the XRD diagrams (Fig. 2) with the change of position of the peak around 5°.

The isotherms corresponding to the Clay/TMOS and Clay/EDAS series are represented in Figs. 3 and 4, respectively. For the Clay/TMOS series, the isotherms evolve from a type IV isotherm (mesoporous solid for the raw clay) to a type I (microporous solid for the Clay/TMOS 3/10)

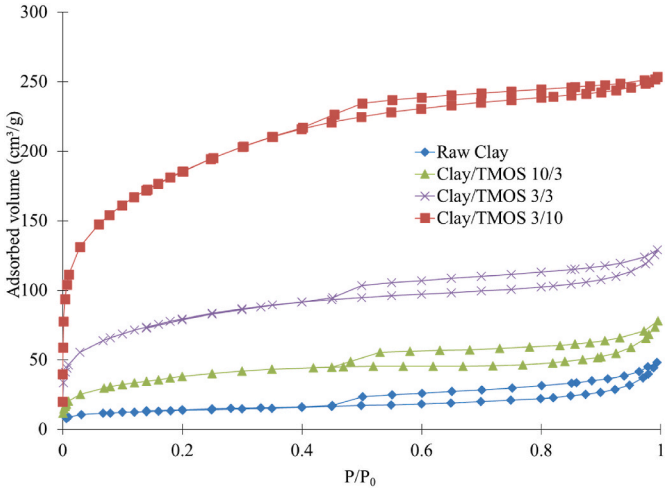

Fig. 3. Nitrogen adsorption–desorption isotherms for (◆) Raw Clay, (▲) Clay/TMOS 10/3, (x) Clay/TMOS 3/3 and (■) Clay/TMOS 3/10 samples.

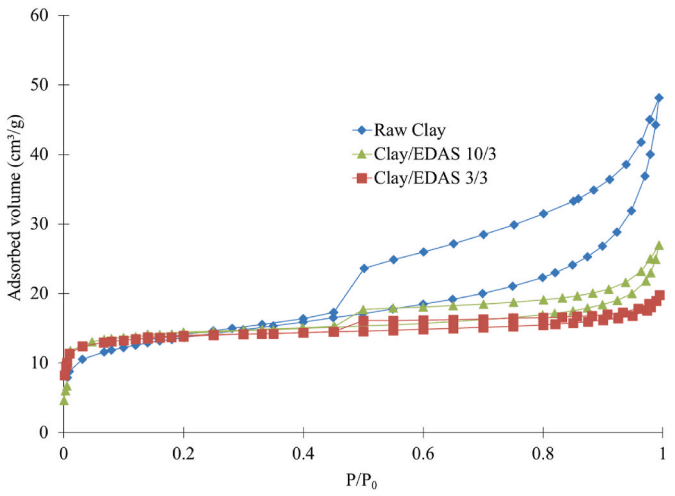

Fig. 4. Nitrogen adsorption–desorption isotherms for (◆) Raw Clay, (▲) Clay/EDAS 10/3 and (■) Clay/EDAS 3/3 samples.

when the amount of TMOS increases compared to the clay. In all samples, a hysteresis is noticed due the presence of mesopores. For the Clay/EDAS series, the shape of the isotherm stays the same, only the volume at saturation decreases due to less mesopores probably filled with EDAS molecules.

A more detailed study of the sample surface was carried out by SEM (Fig. 5). It is observed that the surface of the silica pillared clays by the sol-gel process is considerably affected on some samples as shown in the images in Fig. 5. On the raw material, the typical clay sheets are present; however, on the Clay/TMOS series, the surfaces of the samples are covered with large continuous silica networks giving a rougher aspect of the surface (Fig. 5b and c). These results are in agreement with the high specific surface areas found for the Clay/TMOS series. On the contrary the Clay/EDAS series does not show significant differences with the raw clay sample.

The differences observed in the SEM images, the gelation time during the grafting, XRD patterns and nitrogen adsorption-desorption isotherms in the TMOS and EDAS series can be explain by two different mechanisms in the two series: (i) in the Clay/TMOS series, the addition of TMOS produces amorphous silica network mixed with the clay (Fig. 2) leading to a porous hybrid material (Table 4) where porous silica particles cover the surface of the clay sheets (Fig. 5b, c and 5d); (ii) in the Clay/EDAS series, the EDAS molecules are probably grafted to the surface of the clay producing a continuous dense coating at the surface with similar aspect to the Raw Clay (Fig. 5e and f) reducing the porous volume of the Raw Clay (Table 4) and keeping the same crystallinity of the Raw Clay (Fig. 2) with a displacement of the basal peak.

The formation of both different structures leads to two series of hybrid materials with new surface properties, one with a high surface area containing a lot of silica surface groups and one with silane grafted at the surface containing amine groups. These materials can have interesting adsorption properties due to high porosity or specific amine groups at the surface, their adsorption capacities are explored in the next section.

3.4. Adsorption properties of hybrid samples

The adsorption efficiency of functionalized clays was tested on the removal of 3 model pollutants: fluorescein (FL), malachite green (MG), and brilliant violet diamond (BVD) which are represented in Fig. 6. These pollutants are listed among those generally used in the pesticide and textile industry (Mahy et al., 2019b; Lalonger, 1994; Alderman, 1985). For each pollutant, the evolution of the pollutant concentration over time is estimated with different concentrations of adsorbent materials between 5 and 30 mg of sample for 20 mL of pollutant solution. The initial pH for the three pollutant solutions is 5.3, 6.2, and 7.2 for FL, MG, and BVD, respectively.

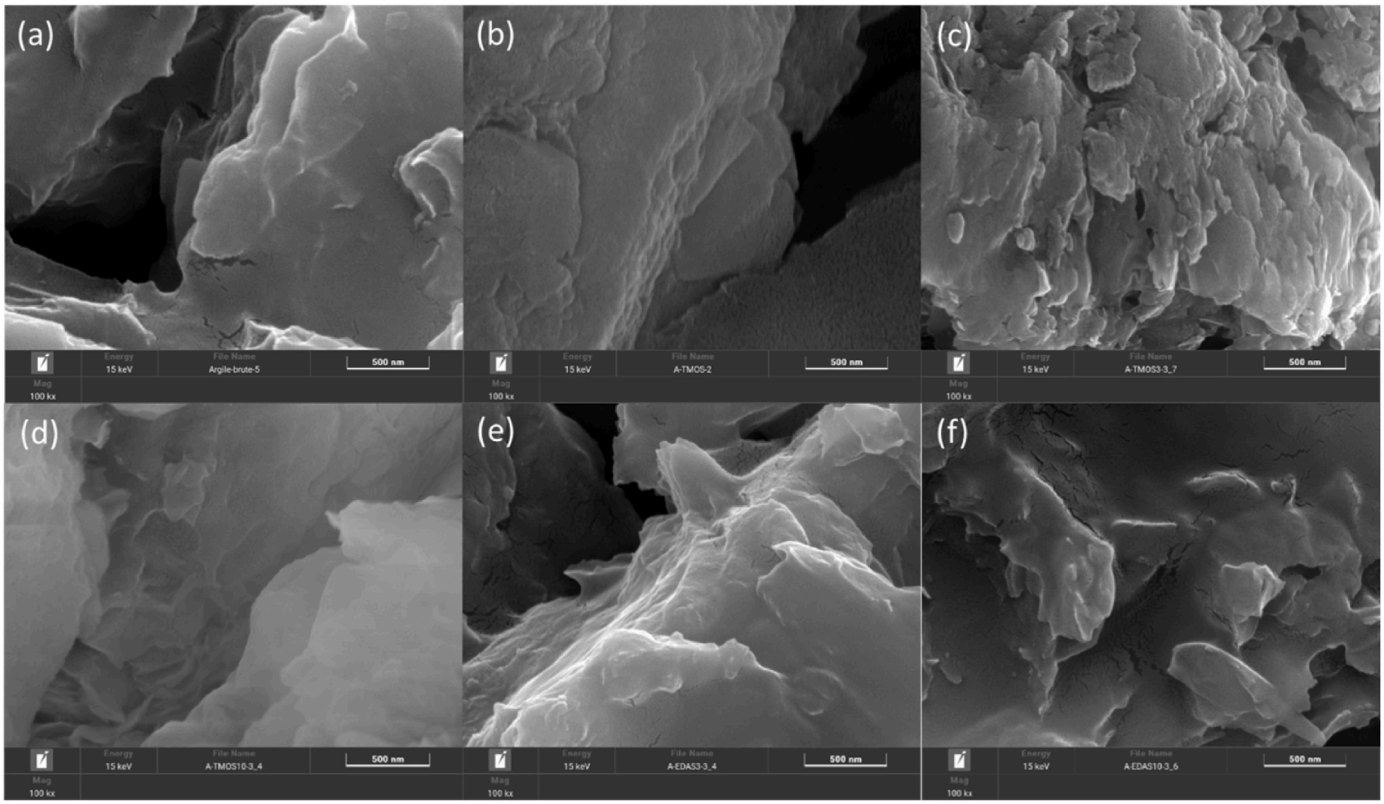

Fig. 5. SEM pictures of (a) Raw Clay, (b) Clay/TMOS 3/10, (c) Clay/TMOS 3/3, (d) Clay/TMOS 10/3, (e) Clay/EDAS 3/3, and (f) Clay/EDAS 10/3 samples.

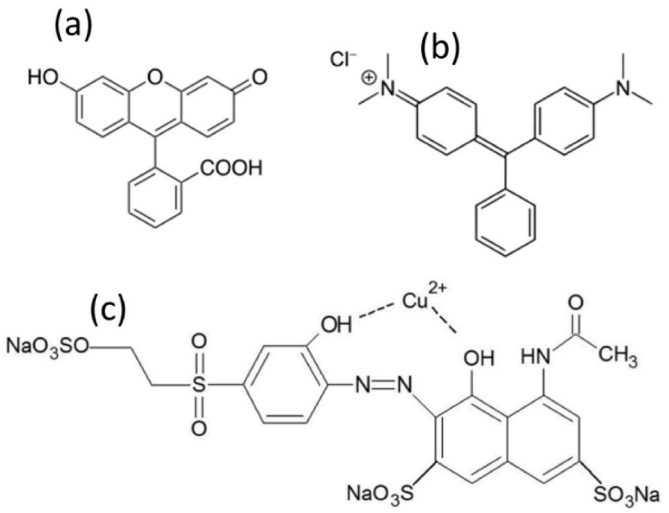

Fig. 6. Molecular structure of (a) fluorescein, (b) malachite green and (c) brilliant violet diamond.

For each sample, the zeta potential and the point of zero charge were measured (Table 4) for a concentration of 1 g/L of sample (it corresponds to the condition with 20 mg of sample). The pH with the different clays is also measured. It will allow to better understand the adsorption phenomenon.

For the fluorescein, Fig. 7 represents the evolution of the concentration (C/C_0) during 1 h for the 6 samples. With the Raw Clay, around 80% of FL are adsorbed during the experiment (Fig. 7a), the modifications with TMOS (Fig. 7b–d) allow to increase the adsorption capacity of the sample leading to a total FL adsorption during the experiments. This modification significantly increases the specific surface area (Table 4). However, the specific surface area is not the only parameter involved in the adsorption process, the nature of the surface groups of the adsorbent plays also a role. For the samples modified with EDAS (Fig. 7e), even if the specific surface area is slightly larger (Table 4), no adsorption occurs during the experiments. The insertion of the ethylenediamine groups of the EDAS have no affinity with FL. It is observed in Table 4, that the introduction of EDAS modifies the surface charge of the Clay/EDAS samples to a more positive value leading to less adsorption of FL.

Both samples modified with EDAS (Clay/EDAS 3/3 and Clay/EDAS 10/3) do not adsorb fluorescein whatever the adsorbent concentration. It is why only one set of point is represented on Fig. 7e.

For the malachite green, Fig. 8 represents the evolution of the concentration (C/C_0) during 1 h for the 6 samples. The raw clay and the

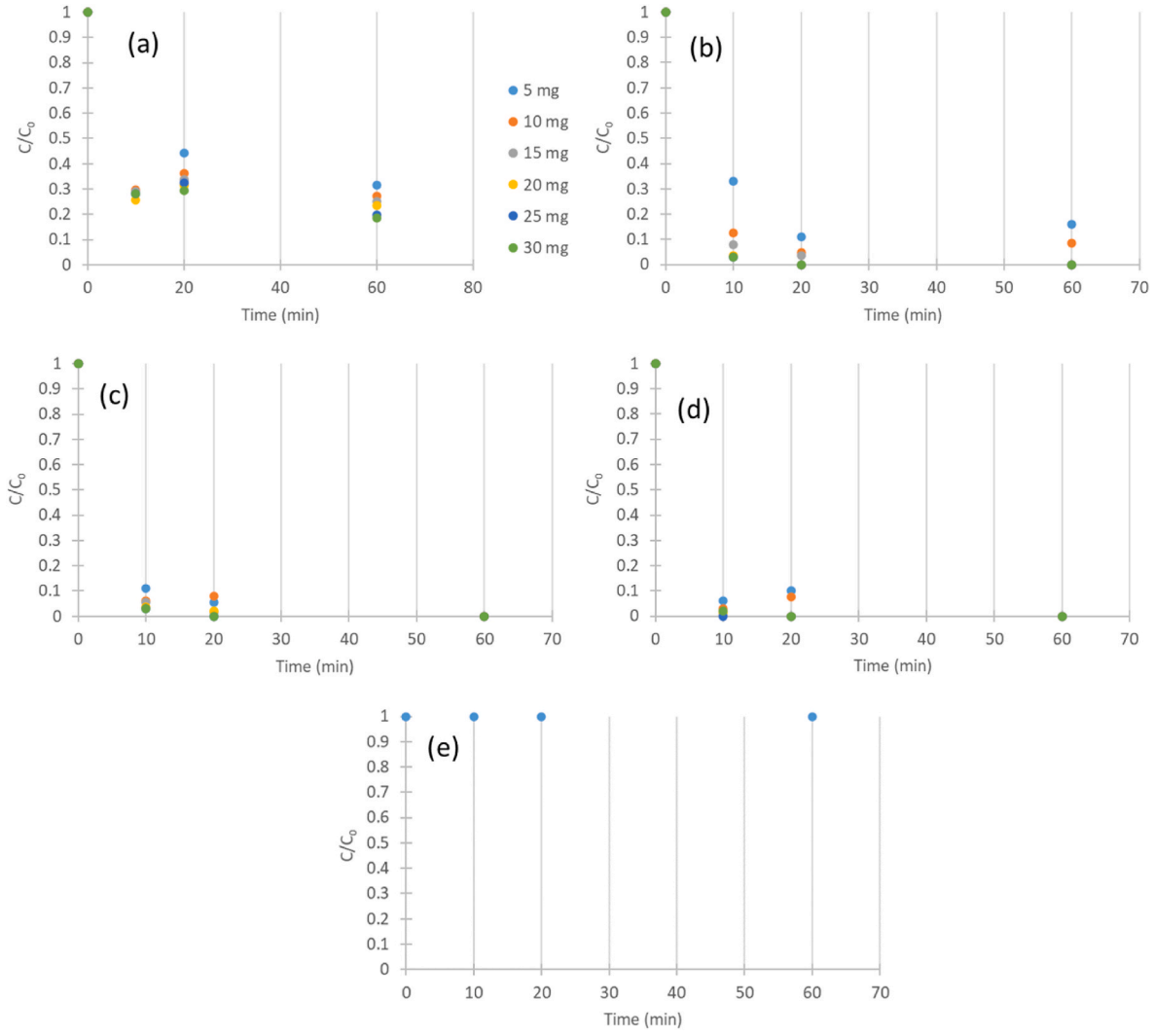

Fig. 7. C/C_0 fluorescein evolution with time for 5–30 mg concentration range for (a) raw clay, (b) Clay/TMOS 10/3, (c) Clay/TMOS 3/3, (d) Clay/TMOS 3/10, and (e) Clay/EDAS 3/3 samples.

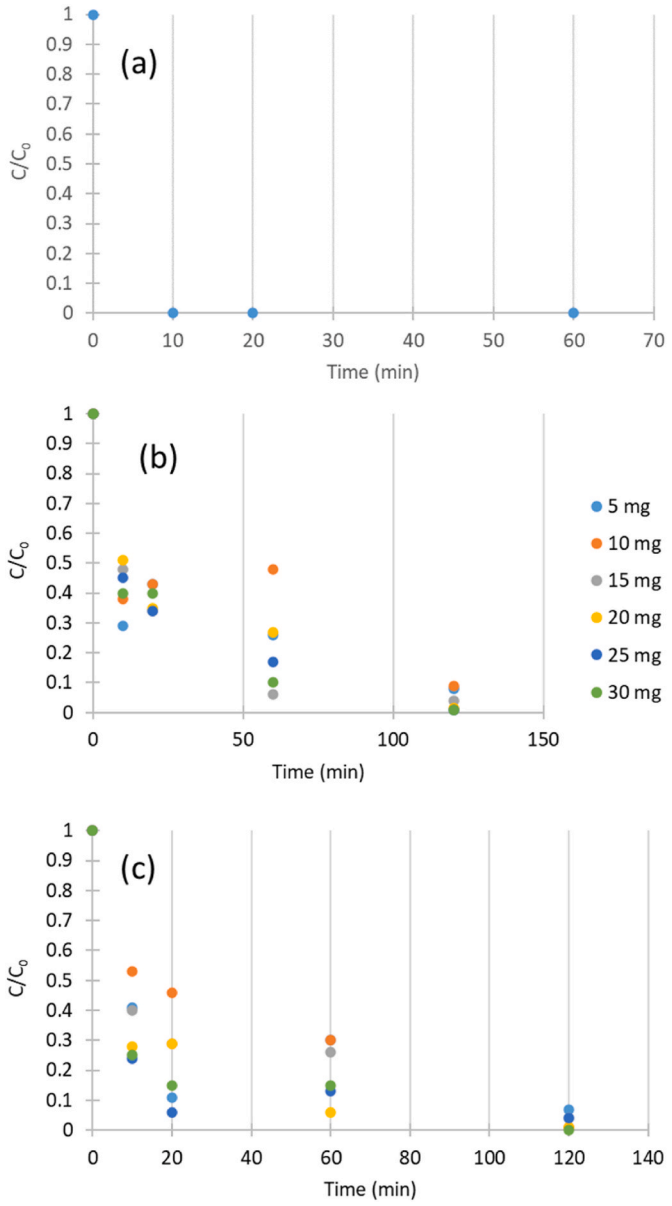

Fig. 8. C/C_0 malachite green evolution with time for 5–30 mg concentration range for (a) raw clay, (b) Clay/EDAS 10/3, and (c) Clay/EDAS 3/3.

samples modified with TMOS adsorb totally MG after 10 min, while the samples modified with EDAS take 2 h to adsorb it totally. The presence of the ethylenediamine groups slows the MG adsorption. The positive charges of the surface of the Clay/EDAS samples (Table 4) seem to slow down the adsorption process.

Raw Clay, and the 3 samples modified with TMOS have the same behavior as represented on Fig. 8a with a complete adsorption of MG after 10 min whatever the adsorbent concentration. It is why only one set of point is represented on Fig. 8a.

For the brilliant violet diamond, the same adsorption behavior is noticed for all samples (Fig. 9) with a fast adsorption of this pollutant in 10 min. For this pollutant, the modification of the clay is not necessary.

Throughout the adsorption of the 3 model pollutants, it is noticed that the surface obtained with samples modified with TMOS brings the most promising adsorbent materials. These materials present the highest specific surface area and a more acidic surface (Table 4). The Clays modified with EDAS results in a more basic surface (Table 4). Depending on the type of pollutant and the surface groups of the adsorbent, very different behaviors can be obtained.

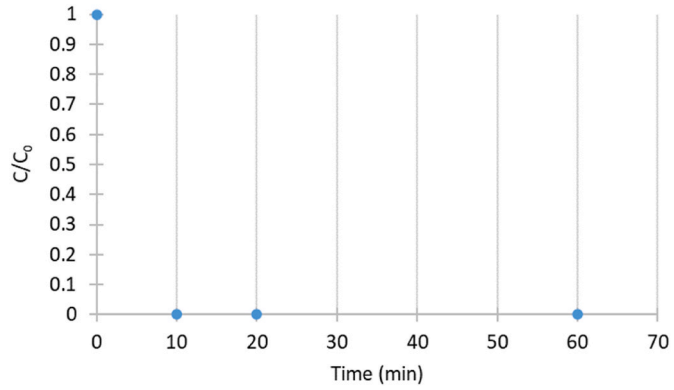

Fig. 9. C/C_0 brilliant violet diamond evolution with time for 5 mg concentration for Raw Clay.

When clay and modified clays are added, the pH of the solution is modified following these tendencies (Table 4): when Clay or Clay/TMOS is added, the pH becomes more acid (between 3.4 and 3.7, Table 4), while with Clay/EDAS, the pH becomes more basic (between 6.1 and 9.2, Table 4). So, the addition of raw Clay and Clay/TMOS samples will result in materials with more acidic sites and/or hydroxyl surface groups that will have more affinity to adsorb on the solid. Contrarily, the Clay/EDAS samples will induce materials with more basic adsorption sites with different adsorption affinity.

All other samples in any concentration have the same the same behavior as represented with a complete adsorption of BVD after 10 min whatever the adsorbent concentration it is why only one set of points is represented on Fig. 9.

3.5. *Comparison with literature*

In Table 5, a comparison of the main results of this study with literature is presented. It is observed that there are many different parameters for one study to another, so a direct comparison is difficult.

Indeed, the materials, the concentration of dye, the time of contact or the design of the adsorption study are different. Nevertheless, it is observed that the modified clays of this study are effective for the removal of three different dyes while usually only one is studied in the other papers. A complete removal of the three pollutants is obtained in a short time (100% in less than 1 h) compared to the other study where at least 2 h are needed. But the dye concentrations of this study (4–20 mg/L) are a bit lower than in other studies (10–240 mg/L). The adsorbent concentration used here (1 g/L) is a bit lower than in other studies (some at 2 (Zaoui et al., 2020), 4 (Ribeiro et al., 2017) or 30 g/L (Shayesteh et al., 2015)).

Zaoui et al. uses also a modified Montmorillonite clay for the removal of MG. 96% is removed after 300 min at a concentration of 2 g/L with an initial MG concentration of 27 mg/L.

4. Conclusion

In this paper, natural raw clay from Cameroon was modified with two silicon alkoxide molecules, tetramethoxysilane (TMOS) and [3-(2-aminoethylamino)propyl]trimethoxysilane (EDAS) in different proportions. The goals of these modifications are to produce hybrid materials with modified surface, higher specific surface area and different surface groups in order to increase their adsorption capacity. The aim is to use these modified clays as organic pollutant adsorbent for water depollution.

The XRD patterns show a dilution of the montmorillonite structure of the raw clay when it is modified with TMOS, while the modification with EDAS keeps its original crystalline structure. When EDAS is introduced, a displacement of the basal peak is observed due to the intercalation of

Table 5
Comparison with literature.

Reference	Materials	Pollutants	Main results
This study	Montmorillonite clay modified with EDAS or TMOS (from Cameroon)	FL (20 mg/L) MG (4 mg/L) BVD (4 mg/L)	100% of adsorption in less than 1 h with the best sample (660 m^2/g – TMOS modified – 1 g/L)
Shayesteh et al. (Shayesteh et al., 2015)	Pumice stone from Iran	MG (10–100 mg/L)	70% of adsorption with 30 g/L of adsorbent
Lesbani et al. (Lesbani et al., 2021)	Keggin Polyoxometalate Intercalated ZnAl Layered Double Hydroxide	MG (40–150 mg/L)	37 mg/g adsorbed on the best sample (2 m^2/g)
Tahir et al. (Tahir et al., 2010)	Montmorillonite clay from Pakistan	MG (10^{-6} to 10^{-3} M) Fast green	97% of removal after 120 min and a concentration of 1 g/L of adsorbent
Zaoui et al. (Zaoui et al., 2020)	natural clay modified with chitosan and thiosulfate (from Algeria)	MG (27 mg/L)	96% of removal after 300 min with 2 g/L of adsorbent
Ribeiro et al. (Ribeiro et al., 2017)	Rice hull from Brazil	BVD (100 mg/L)	73% of removal after 24 h with 4 g/L of adsorbent
Belbel et al. (Belbel et al., 2018)	Homoionic montmorillonite modified with ionic liquid from Wyoming, USA	FL (13–240 µmol/L)	Adsorption capacity of 70 mmol/100 g for the best sample
Pirillo et al. (Pirillo et al., 2009)	Iron oxides (obtained by precipitation method) and chitosan (commercial)	FL (2.5–125 mg/L)	No adsorption on chitosan and very weak on iron oxides
Li et al. (Li et al., 2023)	Anionic sulfonate-functionalized covalent organic framework (synthesized)	FL (10 mg/L)	10% after 120 min with a concentration of 0.25 g/L
Rosli et al. (Rosli et al., 2023)	pineapple peel–based activated carbon from Malaysia	BVD (25 mg/L)	72% after 24 h with a concentration of 0.25 g/L
Anthonysamy et al. (Izwan Anthonysamy et al., 2023)	MgAl/layered double hydroxide supported on rubber seed shell biochar	BVD (25 mg/L)	60% after 24 h with a concentration of 0.8 g/L

the silane. The SEM and BET measurements confirm that two types of materials are produced depending on the silane used: (i) with TMOS, highly porous materials are produced with the formation of silica particles at the surface of the clay with the porosity increasing with the amount of TMOS; (ii) with EDAS, a similar morphology as raw clay is obtained with only a small increase in porosity. In this case, EDAS molecules are grafted at the surface of the clay producing a layer at the surface with new surface ethylenediamine groups.

Both surfaces give different adsorption behaviors on the 3 model pollutants. For the raw clay and the TMOS modified clays, similar adsorption properties are obtained with a better adsorption when the specific surface increases (when TMOS contain increases). In all these samples, similar surface groups are present, the surface groups of the clay and the surface groups of the produced silica (mainly OH groups). A more acidic surface is produced. When clay is modified with EDAS, the adsorption properties change as the surface groups are different due to the grafting of EDAS and a large presence of ethylenediamine groups giving a basic surface. These EDAS modified samples have less affinity with fluorescein and malachite green reducing the adsorption capacity for this kind of pollutants.

The tuning of the raw clay with silane opens the way for the development of highly efficient adsorbent for pollutants in water from natural and inexpensive materials.

Ethical approval

The authors declare that they have no known competing financial interests or personal relationships that could have appeared to influence the work reported in this paper.

Consent to participate

All authors agreed to participate in this work.

Consent to publish

All authors agreed to this version for publication.

CRediT authorship contribution statement

Marlène Huguette Tsaffo Mbognou: Conceptualization, Formal analysis, Investigation, Methodology, Writing – review & editing. **Stéphanie D. Lambert:** Conceptualization, Funding acquisition, Methodology, Project administration, Writing – review & editing. **Ernestine Mimba Mumbfu:** Formal analysis, Investigation. **Joachim Caucheteux:** Funding acquisition, Investigation. **Antoine Farcy:** Formal analysis, Investigation. **Nathalie Fagel:** Funding acquisition, Project administration, Supervision. **Emmanuel Djoufac Woumfo:** Project administration, Supervision. **Julien G. Mahy:** Conceptualization, Formal analysis, Investigation, Methodology, Supervision, Validation, Writing – original draft, Writing – review & editing.

Declaration of competing interest

The authors declare that they have no known competing financial interests or personal relationships that could have appeared to influence the work reported in this paper.

Data availability

Data will be made available on request.

Acknowledgments

Julien G. Mahy and Stéphanie D. Lambert thank the F.R.S.-FNRS for their Postdoctoral Researcher position and Research Director position, respectively. J.G.M. is grateful to the Rotary for a District 2160 grant, to the University of Liège and the FNRS for financial support for a postdoctoral stay at INRS Centre Eau, Terre, Environnement in Québec, Canada. Marlène Huguette Tsaffo Mbognou thanks the PACODEL for her doctoral grant. The authors thank the CARPOR platform of the University of Liège and its manager, Dr. Alexandre Léonard, for the nitrogen adsorption–desorption measurements.

References

Akçay, G., Kilinç, E., Akçay, M., 2009. The equilibrium and kinetics studies of flurbiprofen adsorption onto tetrabutylammonium montmorillonite (TBAM). Colloids Surf. A Physicochem. Eng. Asp. 335, 189–193. https://doi.org/10.1016/j.colsurfa.2008.11.009.

Alderman, D.J., 1985. Malachite green: a review. J. Fish. Dis. 8, 289–298.

Asgari, M., Sundararaj, U., 2018. Silane functionalization of sodium montmorillonite nanoclay: the effect of dispersing media on intercalation and chemical grafting. Appl. Clay Sci. 153, 228–238. https://doi.org/10.1016/j.clay.2017.12.020.

Belbel, A., Kharroubi, M., Janot, J.M., Abdessamad, M., Haouzi, A., Lefkaier, I.K., Balme, S., 2018. Preparation and characterization of homoionic montmorillonite modified with ionic liquid: application in dye adsorption. Colloids Surf. A Physicochem. Eng. Asp. 558, 219–227. https://doi.org/10.1016/j.colsurfa.2018.08.080.

Brinker, G.W., Jeffrey, C., Scherer, 2013. Sol-gel Science: the Physics and Chemistry of Sol-Gel Processing. Academic press.

Carrado, K.A., 2000. Synthetic organo-and polymer-clays: preparation, characterization, and materials applications. Appl. Clay Sci. 17, 1–23. www.elsevier.nlrlocaterclay.

Celis, R., Carmen Hermosín, M., Cornejo, J., 2000. Heavy metal adsorption by functionalized clays. Environ. Sci. Technol. 34, 4593–4599. https://doi.org/10.1021/es000013c.

Claude, V., Mahy, J.G., Geens, J., Courson, C., Lambert, S.D., 2019. Synthesis of Ni/γ-Al2O3-SiO2 catalysts with different silicon precursors for the steam toluene reforming. Microporous Mesoporous Mater. 284, 304–315. https://doi.org/10.1016/j.micromeso.2019.04.027.

De Queiroga, L.N.F., França, D.B., Rodrigues, F., Santos, I.M.G., Fonseca, M.G., Jaber, M., 2019. Functionalized bentonites for dye adsorption: depollution and production of new pigments. J. Environ. Chem. Eng. 7 https://doi.org/10.1016/j.jece.2019.103333.

Dong, J., Zhang, J., 2018. Biomimetic super anti-wetting coatings from natural materials: superamphiphobic coatings based on nanoclays. Sci. Rep. 8 https://doi.org/10.1038/s41598-018-30586-4.

Espínola, J.G.P., Arakaki, L.N.H., De Oliveira, S.F., Da Fonseca, M.G., Campos Filho, J.A. A., Airoldi, C., 2003. Some thermodynamic data of the energetics of the interaction cation-piperazine immobilized on silica gel. Colloids Surf. A Physicochem. Eng. Asp. 221, 101–108. https://doi.org/10.1016/S0927-7757(03)00095-5.

He, H., Duchet, J., Galy, J., Gerard, J.F., 2005. Grafting of swelling clay materials with 3-aminopropyltriethoxysilane. J. Colloid Interface Sci. 288, 171–176. https://doi.org/10.1016/j.jcis.2005.02.092.

He, H., Tao, Q., Zhu, J., Yuan, P., Shen, W., Yang, S., 2013. Silylation of clay mineral surfaces. Appl. Clay Sci. 71, 15–20. https://doi.org/10.1016/j.clay.2012.09.028.

Izwan Anthonysamy, S., Ahmad, M.A., Nasehir, N.K., 2023. Insight the mechanism of MgAl/layered double hydroxide supported on rubber seed shell biochar for Remazol Brilliant Violet 5R removal. Arab. J. Chem. 16 https://doi.org/10.1016/j.arabjc.2023.104643.

Kemgang Lekomo, Y., Mwebi Ekengoue, C., Douola, A., Fotie Lele, R., Christian Suh, G., Obiri, S., Kagou Dongmo, A., 2021. Assessing impacts of sand mining on water quality in Toutsang locality and design of waste water purification system. Clean Eng Technol 2. https://doi.org/10.1016/j.clet.2021.100045.

Komadel, P., Madejová, J., 2006. Chapter 7.1 Acid Activation of Clay Minerals. Dev Clay Sci, pp. 263–287. https://doi.org/10.1016/S1572-4352(05)01008-1.

Lalonger, L., 1994. La transition des colorants naturels aux colorants synthétiques et ses répercussions. Material Culture Review 40.

Lambert, S., Tran, K.Y., Arrachart, G., Noville, F., Henrist, C., Bied, C., Moreau, J.J.E., Wong Chi Man, M., Heinrichs, B., 2008. Tailor-made morphologies for Pd/SiO2 catalysts through sol-gel process with various silylated ligands. Microporous Mesoporous Mater. 115, 609–617. https://doi.org/10.1016/j.micromeso.2008.03.003.

Lesbani, A., Taher, T., Palapa, N.R., Mohadi, R., Mardiyanto, Miksusanti, Arsyad, F.S., 2021. Removal of malachite green dye using keggin polyoxometalate intercalated ZnAl layered double hydroxide. Walailak J. Sci. Technol. 18 https://doi.org/10.48048/wjst.2021.9414.

Li, R., Tang, X., Wu, J., Zhang, K., Zhang, Q., Wang, J., Zheng, J., Zheng, S., Fan, J., Zhang, W., Li, X., Cai, S., 2023. A sulfonate-functionalized covalent organic framework for record-high adsorption and effective separation of organic dyes. Chem. Eng. J. 464 https://doi.org/10.1016/j.cej.2023.142706.

Madejovaʹand, J., Madejovaʹand, M., Komadel, P., 2001. Baseline studies of the clay minerals society source clays: infrared methods. Clay Clay Miner. 49, 410–432. http://pubs.geoscienceworld.org/ccm/article-pdf/49/5/410/3270398/clmn-49-05-0410.pdf?casa_token=bV0nWSPf4BYAAAAA:di3yNEPlB3LnqbzSLitCAQtyepbV1zBF5NSTpvMdV5jK7qQNG8kNGh9rBr2zeBVACfyw-g.

Mahy, J.G., Lambert, S.D., Léonard, G.L.M., Zubiaur, A., Olu, P.Y., Mahmoud, A., Boschini, F., Heinrichs, B., 2016. Towards a large scale aqueous sol-gel synthesis of doped TiO2: study of various metallic dopings for the photocatalytic degradation of p-nitrophenol. J. Photochem. Photobiol. Chem. 329, 189–202. https://doi.org/10.1016/j.jphotochem.2016.06.029.

Mahy, J.G., Claude, V., Sacco, L., Lambert, S.D., 2017. Ethylene polymerization and hydrodechlorination of 1,2-dichloroethane mediated by nickel(II) covalently anchored to silica xerogels. J. Sol. Gel Sci. Technol. 81, 59–68. https://doi.org/10.1007/s10971-016-4272-0.

Mahy, J.G., Paez, C.A., Carcel, C., Bied, C., Tatton, A.S., Damblon, C., Heinrichs, B., Wong Chi Man, M., Lambert, S.D., 2019a. Porphyrin-based hybrid silica-titania as a visible-light photocatalyst. J. Photochem. Photobiol. Chem. 373 https://doi.org/10.1016/j.jphotochem.2019.01.001.

Mahy, J.G., Lambert, S.D., Tilkin, R.G., Wolfs, C., Poelman, D., Devred, F., Gaigneaux, E. M., Douven, S., 2019b. Ambient temperature ZrO_2-doped TiO_2 crystalline photocatalysts: highly efficient powders and films for water depollution. Mater. Today Energy 13. https://doi.org/10.1016/j.mtener.2019.06.010.

Mahy, J.G., Mbognou, M.H.T., Léonard, C., Fagel, N., Woumfo, E.D., Lambert, S.D., 2022. Natural clay modified with ZnO/TiO2 to enhance pollutant removal from water. Catalysts 12. https://doi.org/10.3390/catal12020148.

Mahy, J.G., Carcel, C., Chi Man, M.W., 2023. Evonik P25 photoactivation in the visible range by surface grafting of modified porphyrins for p-nitrophenol elimination in water. AIMS Mater Sci 10, 437–452. https://doi.org/10.3934/matersci.2023024.

Mercier, L., Pinnavaia, T.J., 1998. Heavy metal ion adsorbents formed by the grafting of a thiol functionality to mesoporous silica molecular sieves: factors affecting Hg(II) uptake. Environ. Sci. Technol. 32, 2749–2754. https://pubs.acs.org/sharingguidelines.

Nodehi, R., Shayesteh, H., Kelishami, A.R., 2020. Enhanced adsorption of Congo red using cationic surfactant functionalized zeolite particles. Microchem. J. 153 https://doi.org/10.1016/j.microc.2019.104281.

Paredes-Quevedo, L.C., Castellanos, N.J., Carriazo, J.G., 2021. Influence of porosity and surface area of a modified kaolinite on the adsorption of basic red 46 (BR-46). Water Air Soil Pollut. 232 https://doi.org/10.1007/s11270-021-05450-3.

Park, A.Y., Kwon, H., Woo, A.J., Kim, S.J., 2005. Layered double hydroxide surface modified with (3-aminopropyl) triethoxysilane by covalent bonding. Adv. Mater. 17, 106–109. https://doi.org/10.1002/adma.200400135.

Pirillo, S., Pedroni, V., Rueda, E., Ferreira, M.L., 2009. Elimination of dyes from aqueous solutions using iron oxides and chitosan as adsorbents. Quim. Nova 32. A COMPARATIVE STUDY.

Piscitelli, F., Posocco, P., Toth, R., Fermeglia, M., Pricl, S., Mensitieri, G., Lavorgna, M., 2010. Sodium montmorillonite silylation: unexpected effect of the aminosilane chain length. J. Colloid Interface Sci. 351, 108–115. https://doi.org/10.1016/j.jcis.2010.07.059.

Piscitelli, F., Scamardella, A.M., Romeo, V., Lavorgna, M., Barra, G., Amendola, E., 2012. Epoxy composites based on amino-silylated MMT: the role of interfaces and clay morphology. J. Appl. Polym. Sci. 124, 616–628. https://doi.org/10.1002/app.35015.

Qian, Z., Hu, G., Zhang, S., Yang, M., 2008. Preparation and characterization of montmorillonite-silica nanocomposites: a sol-gel approach to modifying clay surfaces. Phys. B Condens. Matter 403, 3231–3238. https://doi.org/10.1016/j.physb.2008.04.008.

Queiroga, L.N.F., Pereira, M.B.B., Silva, L.S., Silva Filho, E.C., Santos, I.M.G., Fonseca, M. G., Georgelin, T., Jaber, M., 2019. Microwave bentonite silylation for dye removal: influence of the solvent. Appl. Clay Sci. 168, 478–487. https://doi.org/10.1016/j.clay.2018.11.027.

Queiroga, L.N.F., Nunes Filho, F.G., França, D.B., Rodrigues, F., Jaber, M., Fonseca, M.G., 2021. Aminopropyl bentonites obtained by microwave-assisted silylation for copper removal. Colloids Surf. A Physicochem. Eng. Asp. 630 https://doi.org/10.1016/j.colsurfa.2021.127557.

Ribeiro, G.A.C., Silva, D.S.A., Dos Santos, C.C., Vieira, A.P., Bezerra, C.W.B., Tanaka, A. A., Santana, S.A.A., 2017. Removal of Remazol brilliant violet textile dye by adsorption using rice hulls. Polimeros 27, 16–26. https://doi.org/10.1590/0104-1428.2386.

Rosli, N.A., Ahmad, M.A., Noh, T.U., 2023. Nature's waste turned savior: optimizing pineapple peel–based activated carbon for effective Remazol Brilliant Violet dye adsorption using response surface methodology. Inorg. Chem. Commun. 153 https://doi.org/10.1016/j.inoche.2023.110844.

Schreier, M., Regalbuto, J.R., 2004. A fundamental study of Pt tetraammine impregnation of silica: 1. The electrostatic nature of platinum adsorption. J. Catal. 225, 190–202. https://doi.org/10.1016/j.jcat.2004.03.034.

Shayesteh, H., Rahbar-Kelishami, A., Norouzbeigi, R., 2015. Adsorption of malachite green and crystal violet cationic dyes from aqueous solution using pumice stone as a low-cost adsorbent: kinetic, equilibrium, and thermodynamic studies. Desalination Water Treat. 57, 12822–12831. https://doi.org/10.1080/19443994.2015.1054315.

Slaný, M., Jankovič, Ľ., Madejová, J., 2019. Structural characterization of organo-montmorillonites prepared from a series of primary alkylamines salts: mid-IR and near-IR study. Appl. Clay Sci. 176, 11–20. https://doi.org/10.1016/j.clay.2019.04.016.

Song, K., Sandi, G., 2001. Characterization of montmorillonite surfaces after modification by organosilane. Clay Clay Miner. 49, 119–125.

Srivastava, R., Fujita, S., Arai, M., 2009. Synthesis and adsorption properties of smectite-like materials prepared using ionic liquids. Appl. Clay Sci. 43, 1–8. https://doi.org/10.1016/j.clay.2008.06.015.

Tahir, H., Hammed, U., Sultan, M., Jahanzeb, Q., 2010. Batch adsorption technique for the removal of malachite green and fast green dyes by using montmorillonite clay as adsorbent. Afr. J. Biotechnol. 9, 8206–8214. https://doi.org/10.5897/ajb10.911.

Tchanang, G., Djangang, C.N., Abi, C.F., Moukouri, D.L.M., Blanchart, P., 2021. Synthesis of reactive silica from kaolinitic clay: effect of process parameters. Appl. Clay Sci. 207 https://doi.org/10.1016/j.clay.2021.106087.

Tonle, I.K., Ngameni, E., Njopwouo, D., Carteret, C., Walcarius, A., 2003. Functionalization of natural smectite-type clays by grafting with organosilanes: physico-chemical characterization and application to mercury(II) uptake. Phys. Chem. Chem. Phys. 5, 4951–4961. https://doi.org/10.1039/b308787e.

Viville, P., Lazzaroni, R., Pollet, E., Alexandre, M., Dubois, P., 2004. Controlled polymer grafting on single clay nanoplatelets. J. Am. Chem. Soc. 126, 9007–9012. https://doi.org/10.1021/ja048657y.

Wheeler, P.A., Wang, J., Baker, J., Mathias, L.J., 2005. Synthesis and characterization of covalently functionalized laponite clay. Chem. Mater. 17, 3012–3018. https://doi.org/10.1021/cm050306a.

Zaoui, F., Choumane, F.Z., Hakem, A., 2020. Malachite green dye and its removal from aqueous solution by clay-chitosane modified. Mater. Today Proc. 49, 1105–1111. https://doi.org/10.1016/j.matpr.2021.09.487.

Zhou, C.H., Zhao, L.Z., Wang, A.Q., Chen, T.H., He, H.P., 2016. Current fundamental and applied research into clay minerals in China. Appl. Clay Sci. 119, 3–7. https://doi.org/10.1016/j.clay.2015.07.043.